Solar Energy
and Sustainable Development
Refereed, biannual scientific journal issued by
The Libyan Center for Solar Energy Research and Studies

Optimized LSTM Neural Networks Model applied for Solar PV Power Prediction

Itto Ouzouhou[1*], **Abdellah Laazizi**[2], **Khalid Kandoussi**[3], **Rabie EL Otmani**[4].

[1,2]Research Modeling and Multiphysics Engineering Laboratory, *ENSAM,* Moulay Ismail University, Meknes, Morocco.
[3,4]Science Engineer Laboratory for Energy, National School of Applied Sciences, Chouaib Doukkali University, El Jadida, Morocco.

E-*mail:* [1]*Itto.ouzouhou@edu.umi.ac.ma*, [2]*a.laazizi@ensam.umi.ac.ma*
[3]*kkandouss@gmail.com*, [4]*elotmani.r@ucd.ac.ma.*

ARTICLE INFO.

3rd International Conference on Mechanics, Materials, and Energy. (MME-2024)
May 20- 22, 2024
at: International University of Rabat, Morocco.

KEYWORDS

Photovoltaic power, prediction, LSTM neural networks, Weighted Linear Regression.

ABSTRACT

Energy and climate challenges have driven significant growth in solar power generation. However, solar power production is intermittent and unstable, which complicates its integration into power grids. Techniques of forecasting Photovoltaic (PV) energy are needed to ensure its security and cost-effectiveness. This paper deals with the use of artificial intelligence techniques to predict photovoltaic power.

The proposed techniques are Weighted Linear Regression (WLR) and Long Short-Term Memory neural networks (LSTM).

The proposed techniques are Weighted Linear Regression (WLR) and Long Short-Term Memory neural networks (LSTM). The investigated data in this study was obtained from a photovoltaic solar power plant located in a specific geographical area.

The studied parameters are wind speed (WS), ambient temperature (T), relative humidity (RH), irradiance (GHI) and wind direction (WD). The accuracy and ability of the LSTM model to explain data variation were examined by comparing its predictions with those of the WLR model, based on three performance measures: RMSE, MAE and R2. The obtained results show that weighted linear regression produces an acceptable estimation of photovoltaic power, with an $RMSE$ of 0.424, MAE of 0.342, and R^2 of 0.980. However, the LSTM model performs better and has the potential to improve forecast reliability and accuracy, with an $RMSE$ of 0.355, MAE of 0.157, and R^2 of 0.986.

*Corresponding author.

DOI: https://doi.org/10.51646/jsesd.v15iMME.340

تطبيق نموذج شبكات ذاكرة القصيرة الأمد والطويلة للتنبؤ بالقدرة المولدة من الطاقة الشمسية الكهروضوئية

يطو وزوهو، عبد الله العزيزي، خالد قندوسي، ربيع العثماني

ملخص: أدّت التحديات المتعلقة بالطاقة والمناخ إلى تزايد الاعتماد على الطاقة الشمسية نظرًا لما توفره من مزايا بيئية واقتصادية. إلا أن الطابع المتقطع وغير المستقر لإنتاج الطاقة الشمسية يشكّل عائقًا أمام إدماجها السلس في شبكات التزود بالطاقة. ولمواجهة هذا التحدي، تبرز أهمية تقنيات التنبؤ بإنتاج الطاقة الكهروضوئية (PV) لضمان أمان أنظمة الطاقة وتحقيق فعالية اقتصادية أكبر. في هذا السياق، تم توظيف تقنيات الذكاء الاصطناعي لتوقع الطاقة المنتَجة من الألواح الشمسية، وذلك من خلال اعتماد نموذجين: الانحدار الخطي المُرَجّح (WLR)، وشبكات الذاكرة القصيرة الأمد الطويلة (LSTM). وتم استخدام بيانات حقيقية تم جمعها من محطة طاقة شمسية تقع في منطقة جغرافية محددة، مع التركيز على عدد من المتغيرات المؤثرة، وهي: الإشعاع الشمسي (GHI)، درجة حرارة الهواء (T)، الرطوبة النسبية (RH)، سرعة الرياح (WS)، واتجاهه (WD). وقد جرى تقييم دقة كل من النموذجين من خلال ثلاثة مؤشرات للأداء: الجذر التربيعي لمتوسط مربع الخطأ (RMSE)، ومتوسط الخطأ المطلق (MAE) ، ومعامل التحديد (R^2). وقد أظهرت النتائج أن نموذج الانحدار الخطي المُرَجّح يوفر تقديرات مقبولة لإنتاج الطاقة الشمسية، حيث بلغت قيم مؤشرات الأداء: RMSE = 0.424 ، MAE = 0.342 و R^2 = 0.980. في المقابل، أظهر نموذج LSTM أداءً أفضل، حيث حقق RMSE = 0.355، MAE = 0.157 وR^2 = 0.986، مما يدل على قدرته العالية على تحسين دقة وموثوقية التنبؤات.

الكلمات المفتاحية: الطاقة الكهروضوئية، التنبؤ، شبكات ذاكرة القصيرة الأمد والطويلة، الانحدار الخطي المُرَجَّح

1. INTRODUCTION

Among renewable energy sources, solar energy has been recognized as one of the most promising due to its environmentally clean, abundant resources, free availability, and lack of transportation requirements [1, 2]. Within the solar energy sector, photovoltaic (PV) technology has gained the more popularity and widespread use [3, 4]. Since 2002, PV energy generation has grown by twice approximately every two years, with an average annual growth rate of 48% [5]. This increase makes photovoltaic technology the fastest-growing energy technology globally. In 2023, the worldwide installed PV cumulative capacity was estimated at 1500 GW [6].

However, the randomness and intermittency of solar energy, due to rapid and random weather changes, present many challenges for the stability and management of integrated power grids [7-11]. In order to integrate safely any photovoltaic system into smart grids, reliable forecasting methods have become crucial to mitigate adverse effects such as low stability and the impact of photovoltaic power uncertainty. These forecasting methods help solve photovoltaic power planning and modelling issues in energy management systems, thereby improving reliability and maintaining power quality [12, 13].

Numerous studies have focused on predicting photovoltaic power by using various methods designed for high accuracy and minimal complexity. These prediction methods, which utilize historical meteorological data, can be categorized into two main groups: statistical techniques and machine learning techniques [14, 15].

For statistical methods, they include linear regression [16], Auto-Regressive Moving Average (ARMA) model [17, 18], Auto-Regressive Integrated Moving Average (ARIMA) model [19, 20], seasonal ARIMA model [21], and ARIMA with exogenous inputs model [22].

In fact, photovoltaic energy production is predicted by statistical analysis of various input variables to establish a correspondence relationship between input-output data using techniques such as curve fitting, parameter estimation and correlation analysis [23]. These methods are applied to the short-term forecasting of photovoltaic energy generation using historical environmental data obtained from photovoltaic sites [24]. Compared to machine learning methods, statistical models require fewer input data series [25].

In the other side, machine-learning methods require larger datasets for accurate forecasting and offer many advantages in linear, non-linear, and non-stationary data patterns [26, 27]. These intelligent techniques are involved in various aspects of PV system design for modelling, controlling, and monitoring [28]. Due to their ability to efficiently extract high dimensional complex nonlinear features, machine-learning methods have become widely used for predicting PV power output [29]. Several studies have applied machine learning models for PV power forecasting such as Artificial Neural Networks (ANNs), which are developed to predict power production hourly in real grid-connected PV plants using various combinations of time series data, irradiance and ambient temperature as inputs [30]. For example, a Multi-Layer Feed-Forward Neural Network (MLFFNN) model was implemented to forecast PV power 24 hours ahead by utilizing historical PV power data along with geographical and meteorological parameters as inputs [31]. Furthermore, other approaches such as Recurrent Neural Networks (RNN) [32], conventional neural networks (CNN) [33], Support Vector Regression (SVR), Random Forest (RF) [34], and Long-Short Term Memory (LSTM) models [35] were employed to predict PV power, solar irradiance, and cloud cover for standalone microgrids.

In the present study, a Long Short-Term Memory (LSTM) Neural Network data driven model is proposed for forecasting photovoltaic (PV) power generation. The implemented model employs previous meteorological parameters and PV power generation data to accurately predict the future PV power output.

Therefore, to ensure reliable modelling, the proposed LSTM model is verified using various architectures and parameter settings. The obtained optimal LSTM is compared with Weighted Linear Regression (WLR) to evaluate the performance of the model. In addition, it is tested under different weather condition scenarios (sunny and cloudy) to ensure the robustness of the model.

2. MATERIALS AND METHODS

2.1. Data sets and features

In this subsection, the data used in this work was descripted. The historical data includes actual solar power and five weather variables: wind speed (WS), ambient temperature (T), relative humidity (RH), irradiance (GHI) and wind direction (WD). The output power and meteorological parameters were recorded from January 1st, 2014, to January 1st, 2017. To minimize the effects of rapidly changes in meteorological conditions, data were recorded every 5 min [36]. To ensure the integrity and reliability of the dataset, a comprehensive preprocessing procedure was implemented to address both outliers and missing values. Outlier detection and removal were performed using a multivariate filtering technique based on the Mahalanobis

distance, which quantifies the distance of each observation from the multivariate mean while accounting for correlations among variables. Observations with Mahalanobis distances exceeding a specified threshold—typically determined by the chi-square distribution—were identified as outliers and excluded from further analysis.

To address the issue of missing data, linear interpolation was employed as a decomposition strategy. This method estimates missing values by fitting a straight line between the nearest known data points, thereby preserving the temporal continuity and inherent trends within the dataset while minimizing the risk of introducing bias.

2.2. Long-Short-Term Memory Neural Network (LSTM)

The Long Short-Term Memory (LSTM) network is a type of recurrent neural network (RNN) designed to handle both short and long-term dependencies in sequential data more effectively. Unlike traditional RNNs, LSTM networks are trained using backpropagation through time, which mitigates the vanishing gradient problem that often hampers the learning of long-range patterns.

As illustrated in Figure 1, the architecture of an LSTM network is composed of multiple memory cells arranged in layers to process time-series input sequentially. Each of these cells is designed to retain and manage information across time steps using internal gating mechanisms [37].

Each LSTM unit contains a memory cell c_t and a hidden state h_t, which are updated at every time step. As shown in Figure 2, the internal structure of an LSTM unit includes three key gates: the input gate it, the forget gate ft, and the output gate ot. These gates control the flow of information into and out of the cell:

- Input gate ($\boldsymbol{i_t}$): Determines which new information is allowed into the memory cell.
- Forget gate ($\boldsymbol{f_t}$): Controls information from the previous cell state c_{t-1} that should be discarded.
- Output gate ($\boldsymbol{o_t}$): Regulates the memory cell that is exposed to the output.

The LSTM unit combines inputs with learned weights and biases, passing them through sigmoid or tanh activation functions to compute gate activations. The updated cell state is calculated by combining the previous state and the candidate state using the forget and input gates, respectively. The final hidden state h_t is obtained by applying a tanh transformation to the updated cell state and modulating i_t with the output gate activation.

The entire process can be described mathematically as follows (Eq. 1-6) [38-40]:

Input gate:

$$i_t = \sigma_g(W_i x_t + U_i h_{t-1} + b_i) \quad (1)$$

Forget gate:

$$f_t = \sigma_g(W_f x_t + U_f h_{t-1} + b_f) \quad (2)$$

Candidate cell state:

$$\tilde{c}_t = tanh(W_c\, x_t + U_c h_{t-1} + b_C) \quad (3)$$

Cell state update:

$$c_t = f_t \odot c_{t-1} + i_t \odot \tilde{c}_t) \quad (4)$$

Output gate:

$$o_t = \sigma_g(W_O\, x_t + U_O h_{t-1} + b_O \quad (5)$$

Hidden state:

$$h_t = o_t \odot tanh(c_t) \quad (6)$$

Where:

x_t:	input at the current time step,
h_{t-1}, c_{t-1}:	hidden and cell states from the previous time step,
$W *$, $U *$:	input and recurrent weight matrices,
$b *$:	bias terms,
σ_g:	sigmoid activation function,
$tanh$:	hyperbolic tangent function,
$\odot$:	element-wise multiplication.

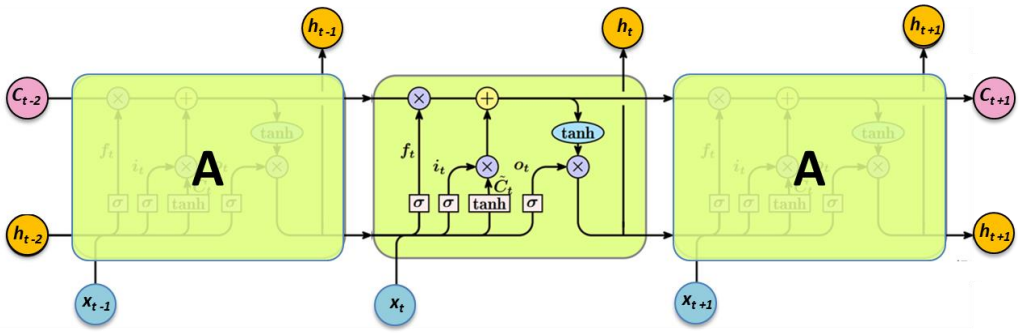

Figure 1. Overview of LSTM interactive layers.

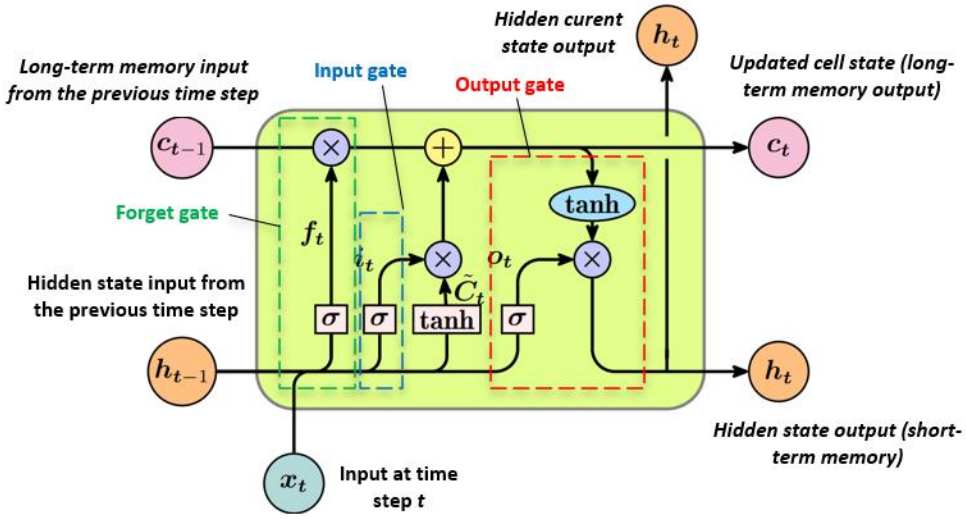

Figure 2. Structural diagram of LSTM unit.

2.3. Performance metrics

Several statistical indicators have been measured to evaluate the performance of the developed models, including Mean Absolute Error (MAE), Root Mean Square Error (RMSE)

and the coefficient of determination (R^2). These can be expressed as follows (Eq.7-9) [41, 42]:

- Mean Absolute Error (MAE):

$$MAE = \frac{1}{N}\sum_{i=1}^{N}|\hat{y}_i - y_i| \quad (7)$$

Where y_i is the measured output value, $\hat{y}_i$ is the predicted value, and N is the number of observations.

- Root Mean Square Error (RMSE):

$$RMSE = \sqrt{\frac{\sum_{i=1}^{N}(\hat{y}_i - y_i)^2}{N}} \quad (8)$$

- Coefficient of Determination (R^2):

$$R^2 = 1 - \frac{\sum_{i=1}^{N}(\hat{y}_i - y_i)^2}{\sum_{i=1}^{N}(\bar{y} - y_i)^2} \quad (9)$$

The flowchart of PV output power prediction using LSTM model is shown in Figure 3:

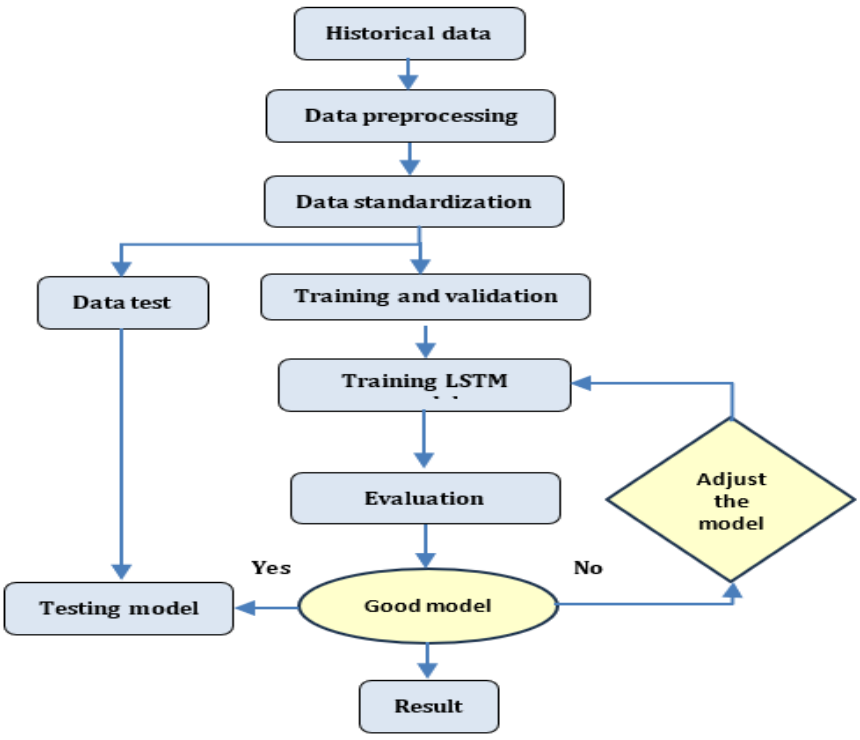

Figure 3. The prediction process of PV output power.

3. RESULTS AND DISCUSSION

3.1. Correlation analysis

In this study, a correlation analysis has been conducted to select the features to be included in the datasets for model training, aiming to create an efficient power output forecaster. Pearson's correlation coefficient has been utilized to assess the degree of relationship between the variables under consideration. Figure 4 presents the results of this correlation analysis in the form of a correlation matrix [43].

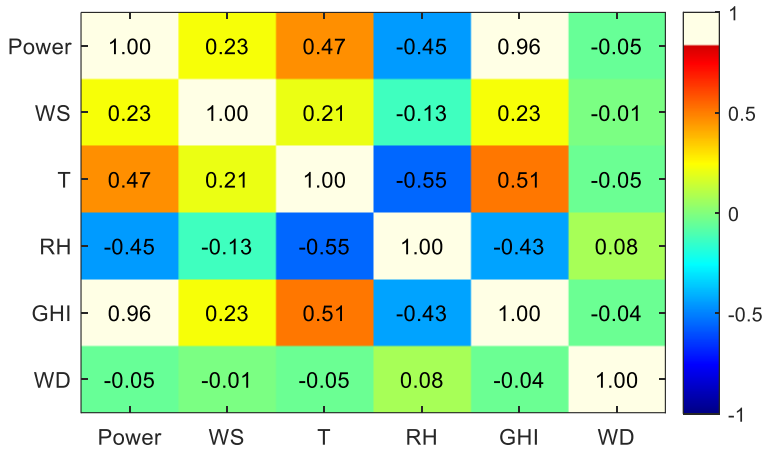

Figure 4. Correlation matrix.

The correlation matrix enables the evaluation of the influence of each variable on the others, as indicated by a color gradient (Figure 4).

A comparative analysis reveals that in the PV output power column, the correlation coefficients for wind speed (WS), ambient temperature (T) and irradiance (GHI) are 0.23, 0.47 and 0.96, respectively. This indicates a positive correlation among these three variables. Conversely, negative correlations were observed between PV output power and relative humidity and wind direction, with scores of -0.45 and -0.05, respectively. Notably, irradiance (GHI) emerged as the most influential variable, while wind direction showed weak correlations.

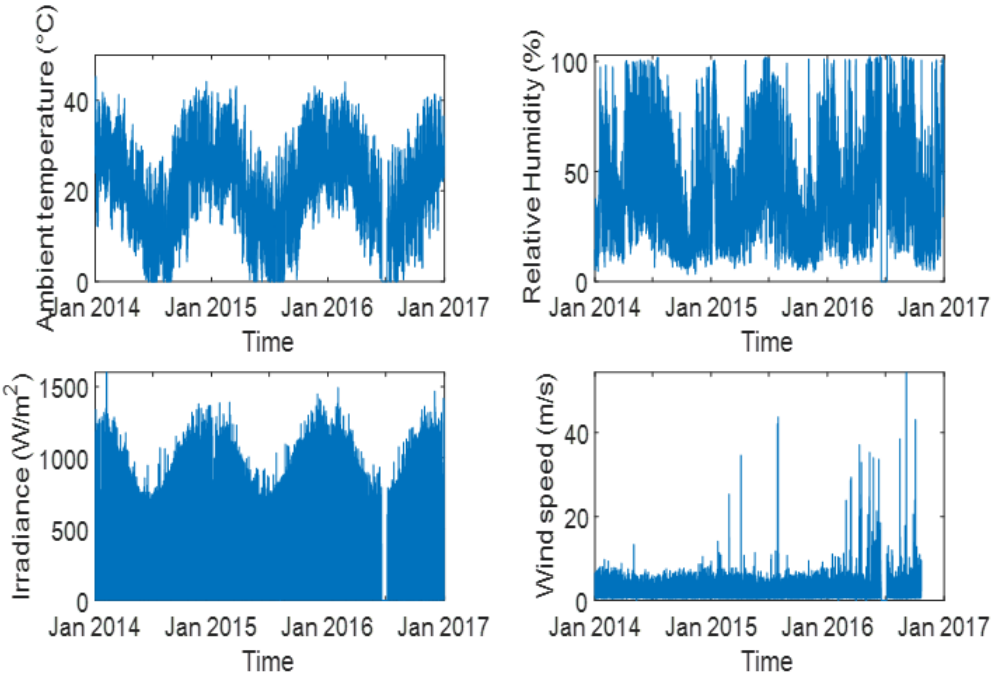

Figure 5. Observed ambient temperature, Irradiance, Wind speed, Relative humidity, Wind direction and Power.

As a result, the input data has been reduced from five parameters to four. Utilizing the correlation matrix is crucial for simplifying model complexity, which subsequently decreases the computational load during training. Based on this analysis, the parameters with significant

effects on power production (wind speed (WS), ambient temperature (T), relative humidity (RH) and irradiance (GHI)) are identified as potential inputs for estimating PV power output.

Therefore, the input variables used in this study, namely the ambient temperature (°C), irradiance (W/m2), wind speed (m/s) and relative humidity (%) of the following data (collected every 5 min) from January 1st, 2014 to January 1st, 2017 are represented in Figure 5.

3.2. PV power forecasting

After processing outliers and missing values, all inputs and the output are rescaled using the min-max normalization technique to map feature data to the range [0, 1]. This is carried out using the following formula [44]:

$$\hat{x} = \frac{x - x_{min}}{x_{min} - x_{max}} \tag{10}$$

Where $\hat{x}$ is the normalized data, x is the original data, and x_{min} and x_{max} denote the minimum and maximum values of a specific feature within the dataset, respectively.

Before setting up the forecasting model, outliers and missing values in the experimental data, resulting from abnormal weather measurement parameters, are removed. The normalized data has been divided into 70%, which is randomly assigned to the training set, 15% to the validation set, and 15% to the test set.

In this study, robustness test has been conducted of the proposed LSTM model. Therefore, the parameter settings and architecture of the models are adjusted to obtain improved forecasting results. Seven models with different architectures and parameter settings are evaluated using the same training data to assess their impact on model performance (Table 1).

Table 1. Seven LSTM models with different architectures and parameter settings.

LSTM Models	LSTM Models parameters				Performance metrics		
	Architecture	Parameter settings					
	LSTM layers	LSTM Units	Batch size	learning rate	RMSE	MAE	R^2
Model 1	1	50	128	0.01	0.46	0.28	0.97
Model 2	1	75	128	0.01	0.53	0.29	0.96
Model 3	2	50.50	128	0.01	0.49	0.31	0.96
Model 4	2	50.75	128	0.01	0.54	0.32	0.96
Model 5	2	75.50	128	0.01	0.49	0.27	0.97
Model 6	1	500	128	0.01	0.48	0.34	0.97
Model 7	1	500	128	0.005	0.49	0.32	0.97

The hyperparameters that can be adjusted include the learning rate and batch size. Additionally, the model architecture can be modified by varying the number of LSTM layers and the number of LSTM units (neurons), with the optimizer set to Adam.

Hyperparameters selection was guided by a trial-and-error procedure, in which multiple configurations were tested and evaluated using performance metrics to identify the optimal parameters.

Table 1 presents the performance metrics of seven LSTM models. As shown in this table, all models demonstrate the good performances, which proves that LSTM model, trained with different architectures and parameter settings, aligns with the actual PV power output. However, model 1 is the best among all models, which has the simplest architecture. The

optimal parameter setting and architecture of this model are summarized in Table 2.

Table 2: Optimal parameters of LSTM Model.

Parameters	Number of LSTM layers	Learning rate	Number of hidden units	Optimizer	Batche size
Value	1	0.01	50	ADAM	128

Figure 6 depicts the measured and predicted PV power values over a week. The predicted values closely match the measured values, indicating the model's ability to accurately forecast short-term PV power output. Minimal deviations between the predicted and actual values reflect the effectiveness of the LSTM model in capturing the complex nonlinear relationships between the input meteorological variables and the PV power output.

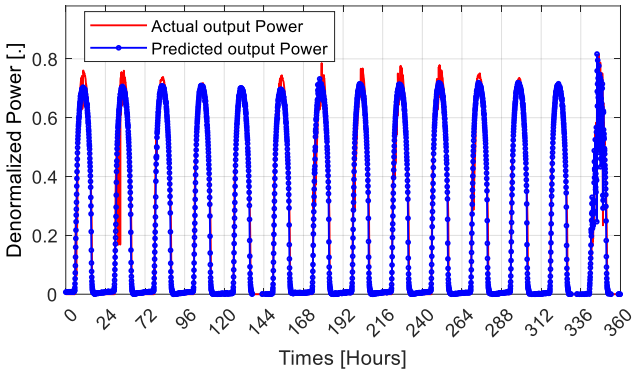

Figure 6. Actual and predicted PV power using the optimized LSTM model.

Overall, the Figure 6 highlights the robustness and accuracy of the LSTM model for predicting PV power, showing its potential for integration into energy management systems to enhance grid stability and efficiency.

Figure 7 presents the frequency distribution of the prediction errors. The range of errors is concentrated between −1 and +1, indicating that the model performs reliably in most cases.

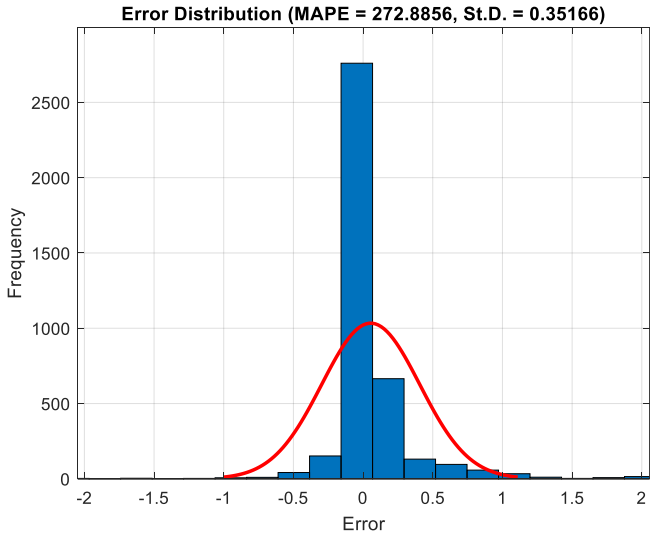

Figure 7. Frequency distribution of the error.

This concentration around zero proposes a high level of predictive accuracy and minimal bias. However, a minimal moderate error remains, which may be attributed to factors such as inherent noise in the data, abrupt changes in temporal dynamics, or the limited capacity of the model to capture certain complex patterns that were not well represented during training.

In addition, the comparison analysis of the LSTM model with the Weighted Linear Regression (WLR) model is shown in Table 3, and the dataset for one week is represented in Figure 8 to directly reflect this comparison.

Figure 8 illustrates the results of comparing the two prediction models (LSTM and WLR) for one week. Results show that the trend of the predicted values for both models is consistent with the real values. However, the degree of correlation between the predicted values and the real values is better for the LSTM model than for the WLR model.

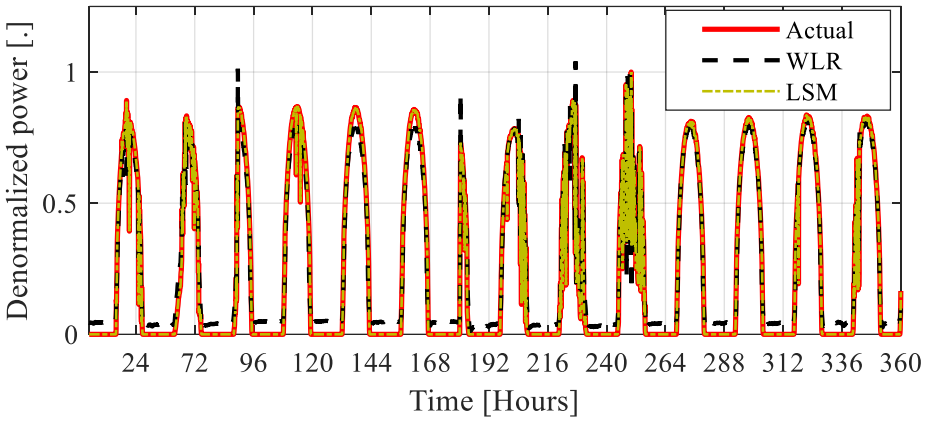

Figure 8: Prediction of PV generation with two models LSTM and WLR.

Furthermore, the obtained LSTM model exceed the WLR model in terms of error metrics. Specifically, the values of RMSE, MAE and R^2 respectively of the LSTM model are significantly improved compared to those obtained by the WLR model. This indicates that the LSTM model achieves superior prediction accuracy compared to the WLR model as shown in Table 3.

Table 3. Comparative analysis between LSTM and WLR.

Parameters	RMSE	MAE	R^2
LSTM	0.355	0.157	0.986
WLR	0.424	0.342	0.980

Additionally, while the WLR model demonstrates good performance, it has limitations when dealing with longer datasets. In contrast, the LSTM model maintains its performance and accuracy even with extended datasets, highlighting its robustness and suitability for long-term forecasting.

Overall, the LSTM model shows a marked improvement over the WLR model in terms of prediction accuracy and reliability, particularly for long-term datasets.

Subsequently, our optimized LSTM models are tested for the two different subsets to explain the influence of weather conditions on the predicted results. These subsets are selected according to the weather conditions: sunny and cloudy, as shown in figures 9 and 10,

respectively. These results show that under the tested subsets, the predicted PV power of the optimized LSTM model is consistent with the change of the actual power. The performance metrics had acceptable values as shown in Table 4, indicating that the optimized LSTM model has good applicability and reliability for different weather conditions. However, the performance metrics of subset 1, corresponding to the sunny week, demonstrate good performance compared to the cloudy subset due to stable weather in the sunny conditions.

Table 4. Performance evaluation in different subsets (sunny and cloudy).

Subsets	RMSE	MAE	R^2
Subset 1	0.254	0.136	0.988
Subset 2	0.540	0.444	0.967

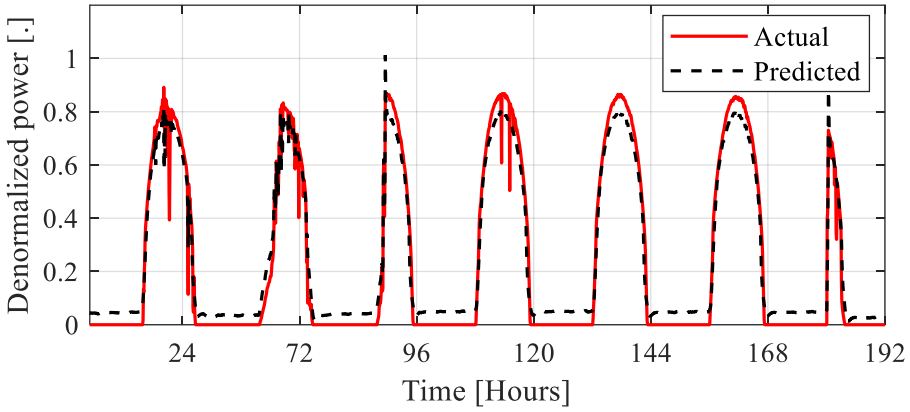

Figure 9: The predicted and actual PV power of the LSTM model in a sunny week.

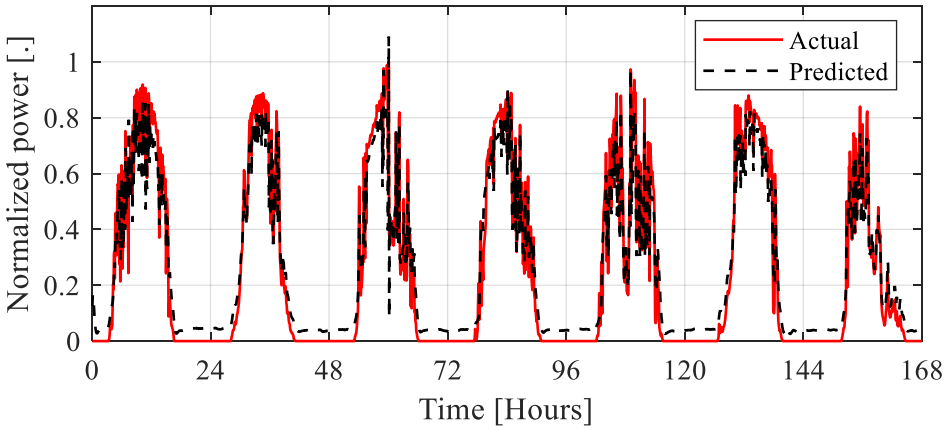

Figure 10: The predicted and actual PV power of the LSTM model in a cloudy week.

In addition, the computational complexity and runtime of both models were assessed to evaluate their practical applicability. Due to its recurrent architecture and nonlinear activation functions, LSTM model incurs higher computational costs. In contrast, WLR remains computationally efficient, making it more suitable for real-time or resource constrained environments. The LSTM model required a significantly longer training time compared to the WLR model, highlighting the higher computational demand associated with deep learning

approaches. However, in the context of photovoltaic (PV) power prediction, where capturing nonlinear and temporal dependencies is essential, the added computational cost of LSTM is justified by its significantly improved forecasting accuracy across all evaluation metrics.

5. CONCLUSIONS:

This study focused on developing and optimizing an LSTM model for predicting solar PV power generation. Initially, a correlation analysis was conducted to assess the impact of different input vectors on PV power prediction. Four input vectors were selected for the input training dataset. The LSTM model was then optimized by adjusting various parameters and its architecture.

The optimal configuration for the predictive model demonstrated excellent generalization capabilities, which make it suitable for application through various datasets. Its performances were evaluated on different subsets (sunny and cloudy) to assess its adaptability to varying scenarios.

Through this optimization process, the LSTM model demonstrated good performance for predicting solar PV power generation and highlight the potential for accurate and reliable long-term forecasting in energy management systems. Furthermore, the LSTM architecture was designed to model complex dependencies and nonlinear relationships through its recurrent structure and internal gating mechanisms. These characteristics enable it to learn long-term dependencies and nonlinear dynamics present in the data, which are commonly observed in real-world time series. In contrast, WLR assumed a linear relationship between the input features and the target variable, which limits its ability for modelling such complexities.

ABBREVIATIONS

The following abbreviations are used in this manuscript:

T	Temperature
HR	Humidity relative
WD	Wind direction
WS	Wind Speed
GHI	Irradiance
RNN	Recurrent Neural Network
$LSTM$	Long Short-Term Memory network
WLR	Weighted Linear Regression
i_t	Input gate
f_t	Forget gate
o_t	Output gate
C_t	Cell state update
C_{t-1}	Cell state from the previous time step
h_t	Hidden state
h_{t-1}	Hidden state from the previous time step
X_t	Input at the current time step
W	Matrices for the respective gates

b	Bias vector
σ	Sigmoid function
$tanh$	Hyperbolic tangent function
MAE	Mean Absolute Error
$RMSE$	Root Mean Square Error
R^2	Coefficient of determination

Author Contributions: I.O.: Conceptualization, methodology, formal analysis, writing—original draft, A.A.: writing—review and editing, resources, validation. K.K.: writing—review and editing, validation. R.E.: writing—review and editing, validation. All authors agreed to publish the current version of the manuscript.
Funding source: This work did not receive any external funding.
Data Availability Statement: Data will be available upon request.
Conflicts of Interest: The authors declare that they have no conflict of interest.

REFERENCES

[1] *E. Rynska, "Review of PV Solar Energy Development 2011–2021 in Central European Countries," Energies, vol. 15, no. 21, p. 8307, 2022.Doi:doi.org/10.3390/en15218307*
[2] *L. B. Chilakapati and T. G. Manohar, "Power Quality Enhancement in a Grid-Integrated Solar-PV System with a Hybrid UPQC Control Strategy," J. Solar Energy and Sustainable Development, J. vol. 13, no. 2, pp. 120–137, 2024.*
[3] *Liu, L., Zhao, Y., Chang, D., Xie, J., Ma, Z., Sun, Q., ... & Wennersten, R., "Prediction of short-term PV power output and uncertainty analysis," J. Applied Energy, vol. 228, pp. 700 711,2018.*
[4] *L. P. S. S. Panagoda, R. A. H. T. Sandeepa, W. A. V. T. Perera, D. M. I. Sandunika, S. M. G. T. Siriwardhana, M. K. S. D. Alwis, and S. H. S. Dilka, "Advancements in Photovoltaic (PV) Technology for Solar Energy Generation," J. Research Technology & Engineering, vol. 4, no. 30, pp. 30–72, 2023.Doi:https://doi.org/10.1016/j.apenergy.2018.06.112.*
[5] *V. Devabhaktuni, M. Alam, S. S. S. R. Depuru, R. C. Green II, D. Nims, and C. Near, "Solar Energy: Trends and Enabling Technologies," J. Renewable and Sustainable Energy Reviews, vol. 19, pp. 555–564, 2013. Doi:doi.org/10.1016/j.rser.2012.11.024*
[6] *A. Jäger-Waldau, "Snapshot of Photovoltaics− May 2023", EPJ Photovoltaics, vol. 14, pp. 23, 2023. Doi: doi.org/10.1051/epjpv/2023016*
[7] *J. Batalla-Bejerano and E. Trujillo-Baute, "Impacts of intermittent renewable generation on electricity system costs", J. Energy Policy, vol. 94, pp. 411-420, 2016. Doi:https://doi.org/10.1016/j.enpol.2015.10.024.*
[8] *M.H. Albadi, "Solar PV Power Intermittency and its Impacts on Power Systems—An Overview", J. Engineering Research, vol. 16, no. 2, 2019. Doi: doi.org/10.24200/tjer.vol16iss2pp142-150.*
[9] *G. Li, H. Wang, S. Zhang, J. Xin, and H. Liu, "Recurrent Neural Networks Based Photovoltaic Power Forecasting Approach," J. Energies, vol. 12, no. 13, p. 2538, 2019. Doi:doi.org/10.3390/en12132538.*
[10] *I. Ali, H. Hadiyanto, and A. Y. Wardaya, "Performance Analysis and Techno-Economic Evaluation of Solar Energy Retrofitting for Coal-Fired Power Plant in Central Kalimantan Province," J. Solar Energy and Sustainable Development, vol. 13, no. 2, pp. 138–150, 2024. Doi:doi.org/10.51646/jsesd.v13i2.205.*
[11] *S. Saeed and T. Siraj, "Global Renewable Energy Infrastructure: Pathways to Carbon*

Neutrality and Sustainability," J. Solar Energy and Sustainable Development, vol. 13, no. 2, pp. 183–203, 2024. Doi:doi.org/10.51646/jsesd.v13i2.243.

[12] K.J. Iheanetu, "Solar Photovoltaic Power Forecasting: A Review", J. Sustainability, vol. 14, no. 24, p. 17005, 2022. Doi:doi.org/10.3390/su142417005.

[13] A. El Hendouzi and A. Bourouhou, "Solar Photovoltaic Power Forecasting," J. Electrical and Computer Engineering, vol. 2020, no. 1, p. 8819925, 2020.

[14] P. Gupta, R. Singh, "PV power forecasting based on data-driven models: a review," int. J. Sustainable Engineering, vol. 14, no. 6, pp. 1733-1755, 2021.Doi:doi.org/10.1080/19397038.2021.1986590.

[15] Al Hazza, M., Attia, H., & Hossin, K., "Solar photovoltaic power prediction using a statistical approach based on analysis of variance," J. Solar Energy and Sustainable Development, vol. 13, no. 2, pp. 45-61, 2024. Doi: doi.org/10.51646/jsesd.v13i2.181.

[16] A. M. Kuriakose, D. P. Kariyalil, M. Augusthy, S. Sarath, J. Jacob, and N. R. Antony, "Comparison of Artificial Neural Network, Linear Regression, and Support Vector Machine for Prediction of Solar PV Power," in 2020 IEEE Pune Section International Conference (PuneCon), pp. 1–6, Dec.2020.Doi:10.1109/PuneCon50868.2020.9362442.

[17] B. Singh and D. Pozo, "A guide to solar power forecasting using ARMA models," in 2019 IEEE PES Innovative Smart Grid Technologies Europe (ISGT-Europe), IEEE, 2019,pp.1-4. Doi: 10.1109/ISGTEurope.2019.8905430.

[18] B. Singh and D. Pozo, "A Guide to Solar Power Forecasting Using ARMA Models," in 2019 IEEE PES Innovative Smart Grid Technologies Europe (ISGT-Europe), pp. 1–4, Sep. 2019, IEEE. Doi: 10.1109/ISGTEurope.2019.8905430.

[19] S. Atique, S. Noureen, V. Roy, V. Subburaj, S. Bayne, and J. Macfie, "Forecasting of Total Daily Solar Energy Generation Using ARIMA: A Case Study," in 2019 IEEE 9th Annual Computing and Communication Workshop and Conference (CCWC), pp. 0114–0119, Jan. 2019, IEEE.Doi:10.1109/CCWC.2019.8666481.

[20] L. Fara, A. Diaconu, D. Craciunescu, and S. Fara, "Forecasting of Energy Production for Photovoltaic Systems Based on ARIMA and ANN Advanced Models," Int. J. Photoenergy, vol. 2021, no. 1, p. 6777488,2021. Doi:doi.org/10.1155/2021/6777488.

[21] Y. Tanoto, G. S. Budhi, and J. C. Widjaya, "Time Series Forecasting for Daily to Monthly Temporal Hourly-based Solar PV Output Power," in 2023 6th International Seminar on Research of Information Technology and Intelligent Systems (ISRITI), pp. 519–523, Dec. 2023, IEEE. Doi: 10.1109/ISRITI60336.2023.10467972.

[22] Y. Li, Y. Su and L. Shu, "An ARMAX model for forecasting the power output of a grid-connected photovoltaic system", J. Renewable Energy, vol. 66, pp. 78-89, 2014.Doi:doi.org/10.1016/j.renene.2013.11.067.

[23] K. J. Iheanetu, "Solar Photovoltaic Power Forecasting: A Review," J. Sustainability, vol. 14, no. 24, p. 17005, 2022. Doi: doi.org/10.3390/su142417005.

[24] K, Wang., Qi, X., & Liu, H., "A comparison of day-ahead photovoltaic power forecasting models based on deep learning neural network," J. Applied Energy, vol. 251, p. 113315,2019.Doi:doi.org/10.1016/j.apenergy.2019.113315.

[25] U. K. Das, K. S. Tey, M. Seyedmahmoudian, S. Mekhilef, M. Y. I. Idris, W. Van Deventer, et al., "Forecasting of Photovoltaic Power Generation and Model Optimization: A Review," J. Renewable and Sustainable Energy Reviews, vol. 81, pp. 912–928, 2018. Doi:doi.org/10.1016/j.rser.2017.08.017.

[26] K. G. Nisha and K. Sreekumar, "A Review and Analysis of Machine Learning and Statistical Approaches for Prediction," in 2017 International Conference on Inventive Communication and Computational Technologies (ICICCT), pp. 135–139, IEEE, Mar.2017.Doi:10.1109/ICICCT.2017.7975174.

[27] D, Su., Batzelis, E., & Pal, B., "Machine learning algorithms in forecasting of photovoltaic power generation," in 2019 International Conference on Smart Energy Systems and Technologies (SEST), pp. 1–6, IEEE, Sept. 2019. Doi:10.1109/SEST.2019.8849106.

[28] A. Youssef, M. El-Telbany and A. Zekry, "The role of artificial intelligence in photovoltaic systems design and control: A review", J. Renewable and Sustainable Energy Reviews, vol. 78, pp. 72-79, 2017. Doi: doi.org/10.1016/j.rser.2017.04.046.

[29] D. Su, E. Batzelis, and B. Pal, "Machine Learning Algorithms in Forecasting of Photovoltaic Power Generation," in 2019 International Conference on Smart Energy Systems and Technologies (SEST), pp. 1–6, IEEE, Sep. 2019. Doi: 10.1109/SEST.2019.8849106.

[30] M. AlShafeey and C. Csáki, "Evaluating Neural Network and Linear Regression Photovoltaic Power Forecasting Models Based on Different Input Methods," J. Energy Reports, vol. 7, pp. 7601–7614, 2021. ANN. Doi:doi.org/10.1016/j.egyr.2021.10.125.

[31] AlShafeey M, Csáki C. 2021. Evaluating neural network and linear regression photovoltaic power forecasting models based on different input methods. Energy Reports. 7:7601-7614. Doi: doi.org/10.1016/j.egyr.2021.10.125.

[32] B.H. Vu and I.Y. Chung, "Optimal generation scheduling and operating reserve management for PV generation using RNN-based forecasting models for stand-alone microgrids", J. Renewable Energy, vol. 195, pp. 1137-1154,2022. Doi: doi.org/10.1016/j.renene.2022.06.086.

[33] V. Suresh, P. Janik, J. Rezmer and Z. Leonowicz, "Forecasting solar PV output using convolutional neural networks with a sliding window algorithm," J. Energies, vol. 13, no. 3, p. 723, 2020. Doi: doi.org/10.3390/en13030723

[34] J. Zeng and W. Qiao, "Short-term solar power prediction using a support vector machine," J. Renewable Energy", vol. 52, pp. 118-127,2013. Doi:doi.org/10.1016/j.renene.2012.10.009.

[35] D. Niu, K. Wang, L. Sun, J. Wu and X. Xu, "Short-term photovoltaic power generation forecasting based on random forest feature selection and CEEMD: A case study," J. Applied Soft Computing, vol. 93, pp. 106389, 2020. Doi: doi.org/10.1016/j.asoc.2020.106389.

[36] DKA Solar Center. Available online: https://www.dkasolarcentre.com.au (accessed on 04 April 2023).

[37] Van Houdt, G., Mosquera, C., & Nápoles, G., "A review on the long short-term memory model," J. Artificial Intelligence Review, vol. 53, no. 8, pp. 5929-5955, 2020. Doi: 10.1007/s10462-020-09838-1.

[38] Malashin, I., Tynchenko, V., Gantimurov, A., Nelyub, V., & Borodulin, A., "Applications of Long Short-Term Memory (LSTM) networks in polymeric sciences: A review," Polymers, vol. 16, no. 18, pp. 2607, 2024. Doi: 10.3390/polym16182607.

[39] Wang, L., Liu, Y., Li, T., Xie, X., & Chang, C., "Short-term PV power prediction based on optimized VMD and LSTM," J. IEEE Access, vol. 8, pp. 165849-165862, 2020. Doi: 10.1109/ACCESS.2020.3022246.

[40] Gao, H., Qiu, S., Fang, J., Ma, N., Wang, J., Cheng, K., et al., "Short-term prediction of PV power based on combined modal decomposition and NARX-LSTM-LightGBM," J. Sustainability, vol. 15, no. 10, pp. 8266, 2023. Doi: https://doi.org/10.3390/su15108266.

[41] S. Theocharides, G. Makrides, G.E. Georghiou and A. Kyprianou, "Machine learning algorithms for photovoltaic system power output prediction", in 2018 IEEE International Energy Conference (ENERGYCON), pp. 1-6, IEEE, 2018. Doi: 10.1109/ENERGYCON.2018.8398737.

[42] Luo, X., Zhang, D., & Zhu, X., "Deep learning based forecasting of photovoltaic power generation by incorporating domain knowledge," J. Energy, vol. 225, pp. 120240, 2021.Doi:doi.org/10.1016/j.energy.2021.120240.

[43] Mitrentsis, G., & Lens, H., "An interpretable probabilistic model for short-term solar power forecasting using natural gradient boosting," J. Applied Energy, vol. 309, pp. 118473, 2022. Doi:doi.org/10.1016/j.apenergy.2021.118473.

[44] R. Ahmed, V. Sreeram, Y. Mishra and M.D Arif, "A review and evaluation of the state-of-the-art in PV solar power forecasting: Techniques and optimization", J. Renewable and Sustainable Energy Reviews, vol. 124, pp. 109792,2020.Doi:doi.org/10.1016/j.rser.2020.109792.